



# Hydroxylamine amplified gold nanoparticle-based aptameric system for the highly selective and sensitive detection of platelet-derived growth factor

Ping Wang, Yinhuan Song, Yanjun Zhao, Aiping Fan\*

Tianjin Key Laboratory for Modern Drug Delivery & High-Efficiency, School of Pharmaceutical Science and Technology, Tianjin University, Tianjin 300072, People's Republic of China

## ARTICLE INFO

### Article history:

Received 30 August 2012

Received in revised form

25 October 2012

Accepted 28 October 2012

Available online 2 November 2012

### Keywords:

Aptamer

PDGF-BB

Chemiluminescent immunoassay

Gold nanoparticles

Hydroxylamine

## ABSTRACT

This study developed a sensitive and selective aptamer-based chemiluminescent (CL) method for the determination of platelet-derived growth factor (PDGF)-BB using hydroxylamine enlarged gold nanoparticles (Au NPs). Rabbit anti-human PDGF-BB polyclonal antibody was covalently coupled on the 96-well plate that offers reactive N-oxy succinimide ester (referred to as NOS group) surface. In the presence of target protein, the biotinylated aptamer was captured on the 96-well plate forming an antibody/PDGF-BB/biotinylated aptamer sandwiched complex, which was followed by the assembly of streptavidin coated Au NPs (streptavidin-gold). Au NPs assembled on the surface of 96-well plate reacted with  $\text{HAuCl}_4$  and  $\text{NH}_2\text{OH}$ , which enabled the catalytic deposition of gold metal onto the Au NPs surfaces. A huge number of  $\text{Au}^{3+}$  ions were released from the hydroxylamine enlarged Au NPs after oxidative gold metal dissolution, which was determined by a simple and sensitive luminol CL reaction. The results showed that the detection limit of the assay is 60 pM of PDGF-BB (corresponding to 6 fmol in a 100  $\mu\text{L}$  volume), which compares favorably with those of other PDGF-BB detection techniques. In addition, this aptameric CL biosensor demonstrated extraordinary specificity. And PDGF-BB has been determined in diluted serum indicating the applicability of this assay.

© 2012 Elsevier B.V. All rights reserved.

## 1. Introduction

Nucleic-acid aptamers are the synthetic single-strand nucleic acids with high specificity and affinity to certain targets ranging from small molecules, proteins to cells [1,2]. Aptamers share similar identification principle for targets with antibodies. In contrast to antibodies, aptamers have many salient features such as chemical stability, high level of both specificity and affinity, ease of synthesis, and flexibility in labeling at a desired site without a loss of activity [3]. Recently, various aptamer-based biosensors have been developed including fluorescence [4,5], electrochemistry [6–8], surface-enhanced Raman scattering [9], quartz crystal microbalance [10], and colorimetric technology etc [11–13]. In these aptamer-based biosensors, CL sensors are highly promising due to the high sensitivity, relatively simple and low costs of instrumentation.

PDGF is a growth factor protein found in human platelets; it can assemble in at least three isoforms: PDGF-AB, PDGF-AA, and PDGF-BB [14]. Among these forms, PDGF-BB has been directly implicated in the cell transformation process and tumor growth and progression. In common practice, its detection is often based on an antigen–antibody reaction and a typical example is

enzyme-linked immunosorbent assay (ELISA). However, the assay suffers from low sensitivity and poor repeatability, as well as tedious marking process and short shelf life of secondary antibodies. Lately several new approaches by employing aptamer as recognition element have been developed [15–19]. For example, Yu et al. developed an electrochemical immunosensor to detect PDGF-BB using polyclonal antibody as the capturing probe and a polymerase-extended long strand circular DNA as the detection probe [20]. Li et al. reported a colorimetric assay system for PDGF-BB detection employing DNA aptamer coupled to rolling cycle amplification (RCA) [21]. These methods significantly improved the detection sensitivity. However, the disadvantage is that it depends on the enzymes, and the processes required to prepare circular oligomer templates are time-consuming and costly [22]. In preference to the enzyme-based methods, Au NPs are particularly attractive in bioassay by virtue of their facile synthesis, large specific surface area, high chemical stability, and biocompatibility [23,24]. As an amplification tag, Au NPs have been the subject of research directed at gene analysis and antibody or antigen detection [25].

In the current study, an aptamer-based CL assay using hydroxylamine amplified Au NPs was developed for the determination of PDGF-BB. The strategy comprised the implementation of antibody-based capture, aptamer-based sandwich detection, and a  $\text{HAuCl}_4$ – $\text{NH}_2\text{OH}$  redox reaction-based catalytic enlargement of assembled Au NP probes, which was followed by an acid

\* Corresponding author. Tel./fax: +86 22 27404498.  
E-mail address: [aipingfan1980@163.com](mailto:aipingfan1980@163.com) (A. Fan).

dissolution and luminol CL detection of the  $\text{Au}^{3+}$  released from the enlarged Au NPs. The new CL aptameric assay combines the inherent signal amplification of gold dissolution analysis with hydroxylamine reduction-based amplification reaction. This CL detection system exhibits high sensitivity and extraordinary specificity. The optimization and attractive performance characteristics of the new CL detection of PDGF-BB are reported in the following sections.

## 2. Experimental

### 2.1. Chemicals

All chemicals were of analytical reagent grade and were used as received. Water was prepared using a Milli-XQ equipment. Rabbit anti-human PDGF-BB polyclonal antibody was purchased from Biosynthesis Biotechnology Co., Ltd. (Beijing, China). Recombinant human PDGF-BB, PDGF-AA, and PDGF-AB were obtained from Peprotech Inc. (New Jersey, USA). Hemoglobin, bovine serum albumin (BSA), calmodulin and casein were purchased from Sigma-Aldrich (St. Louis, MO). Cytochrome C and human serum were obtained from Puboxin Biotechnology Co., Ltd. (Beijing, China). Hydroxylamine, chlorauric acid, Tween 20 and other chemical reagents were obtained from Sinopharm Chemical Reagent Co., Ltd. (Beijing, China). Luminol was purchased from Alfa Aesar (Tianjin, China). Citrate-stabilized Au NPs (13-nm and 44-nm diameter) were prepared according to the methods described in the literature [26,27]. ATP and aptamer labeled with biotin at 3'-end was acquired from Sangon Biological Engineering Technology & Service Co., Ltd. (Shanghai, China) with sequences as follows:

5'-TACTCAGGGCACTGCAAGCAATTGTGGTCCCAATGGGCTGAG-TATTTTTT-biotin-3'

### 2.2. Apparatus

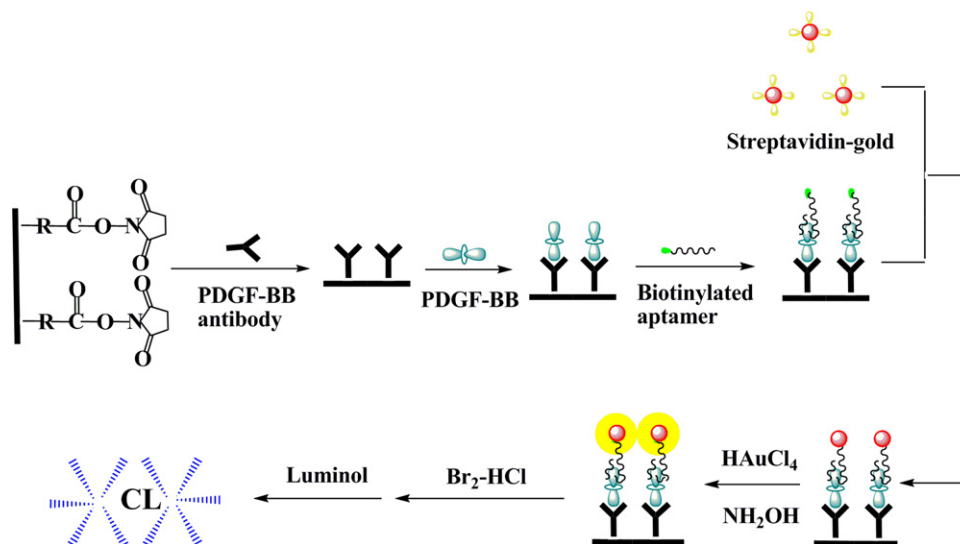
CL measurements were performed with a BPCL chemiluminescence analyzer (Beijing, China). The hydrodynamic sizes of Au NPs were evaluated by a Zetasizer Nano ZS system (Malvern Instruments Ltd., Worcestershire, UK).

### 2.3. Preparation of streptavidin-gold

Streptavidin-gold was prepared via slightly modifying a previous published method [28]. The streptavidin (10% more than the minimum amount, which was determined using a flocculation test) was added to 1 mL colloidal gold suspension (pH 7.0, adjusted by 0.1 M  $\text{K}_2\text{CO}_3$ ) followed by incubation at room temperature for 30 min. The conjugate was centrifuged at 4 °C for 60 min (25,000 g and 14,000 g for Au NPs with a size of 13 nm and 44 nm, respectively). After carefully removing the upper solution, the red soft sediment was resuspended in PBS buffer solution (0.01 M phosphate-buffered saline containing 0.14 M NaCl and 3 mM KCl). The final volume was one-tenth of the volume of original Au NPs. The addition of BSA (0.1%) and  $\text{NaN}_3$  (0.05%) allow storage of streptavidin-gold at 4 °C for several days.

### 2.4. The assay procedure of detecting PDGF-BB

In a typical experiment, rabbit anti-human PDGF-BB polyclonal antibody was diluted to  $1 \text{ ng } \mu\text{L}^{-1}$  using coupling buffer (0.05 M  $\text{Na}_2\text{HPO}_4$ - $\text{NaH}_2\text{PO}_4$ , pH 8.5) and the diluted antibody was allocated into the wells of 96-well plate (100  $\mu\text{L}$  per well) which offers reactive NOS group at plate surface. Following an incubation for 60 min with gentle mixing at 37 °C, the wells were rinsed three times with washing buffer (7 mM Tris, 0.17 M NaCl and 0.05% Tween 20, pH 8.0). After removing the solution, 200  $\mu\text{L}$  of Tris (10 mM in coupling buffer) was added into each well of 96-well plate and incubated at 37 °C for another 60 min to block the remaining NOS groups, and then the wells were rinsed with washing buffer. After discarding the solution, different amount of PDGF-BB in PBSM (0.01 M phosphate-buffered saline, 0.14 M NaCl, 3 mM KCl and 2 mM  $\text{MgCl}_2$ , pH 7.4) was added into each well (100  $\mu\text{L}$  per well), and the resultant mixture was incubated at 37 °C with gentle mixing. After 60 min, the solution was taken off and the wells were rinsed again with the washing buffer. 20 pmol of biotinylated aptamer in buffer R (0.02 M Tris, 0.14 M NaCl, 5 mM KCl, 1 mM  $\text{CaCl}_2$  and 2 mM  $\text{MgCl}_2$ , pH 7.0) was then added into each well following an incubation for 40 min with gentle mixing at 37 °C, the wells were rinsed in triplicate with buffer RT (buffer R containing 0.05% Tween 20). 100  $\mu\text{L}$  of streptavidin-gold (0.464 nM in buffer R) was then added and incubated at 37 °C for 30 min. The wells were rinsed three times with buffer RT, and the



**Scheme 1.** Schematic representation of CL assay for PDGF-BB detection using biotinylated aptamer and hydroxylamine enlarged Au NPs as the recognition element and label, respectively.

Au NPs that assembled on the surface of 96-well plate were catalytically enlarged in the presence of 0.5 mM  $\text{NH}_2\text{OH}$  and 1 mM  $\text{HAuCl}_4$  at room temperature for 4 min, and then the wells were rinsed three times with buffer RT. After carefully removing the rinsing solution, 200  $\mu\text{L}$  of gold metal oxidative solution (final concentration was 0.01 M  $\text{HCl}$ –0.4 mM  $\text{Br}_2$ ) was pipetted into the microwells and reacted for 10 min. The resultant mixture was placed in the water bath at 60  $^\circ\text{C}$  for 27 min; 60  $\mu\text{L}$  of the solution was transferred into 14  $\times$  40 mm glass tubes containing 100  $\mu\text{L}$   $5 \times 10^{-6}$  M luminol (in 0.75 M  $\text{NaOH}$ ) and the CL signal was then displayed in the CL analyzer ( $n=3$ ).

### 3. Results and discussion

#### 3.1. Detection scheme

The principle of CL aptameric immunosensor of PDGF-BB with hydroxylamine amplification is presented (Scheme 1). Hydroxylamine enlarged Au NPs were used to indicate the presence of PDGF-BB that was captured on the surface of 96-well plate by the formation of an antibody/PDGF-BB/biotinylated aptamer sandwiched complex. In a typical experiment, the detection includes four steps: (1) rabbit anti-human PDGF-BB polyclonal antibody is covalently coupled on the 96-well plate that offers the reactive NOS group, followed by an incubation with target protein and biotinylated aptamer to form a ternary complex; (2) the biotinylated ternary complex reacts with streptavidin–gold; (3) Au NPs that assembled on the surface of 96-well plate reacted with  $\text{HAuCl}_4$  and  $\text{NH}_2\text{OH}$ , and then gold metal is catalytically deposited onto the surfaces of the Au NPs; and (4) the gold metal contained in the bound phase is dissolved in an oxidative  $\text{HCl}$ – $\text{Br}_2$  solution, and the gold ions thus released into solution are quantitatively measured by the  $\text{Au}^{3+}$  catalyzed luminol CL reaction. The CL signal is proportionally correlated to the amount of PDGF-BB in the standard or sample.

#### 3.2. Optimization of assay conditions for the determination of PDGF-BB

Several parameters were investigated systematically in order to establish optimal conditions for the CL detection of PDGF-BB, including the amount of PDGF-BB antibody and biotinylated aptamer, the type of blocking material, the concentration of streptavidin–gold, and hydroxylamine amplification conditions. A series of three repetitive measurements of PDGF-BB solution yielded reproducible signals in each condition. First, as shown in Fig. 1, the ratio of signal and blank (referred to as signal/noise ratio) increased rapidly with the increase of PDGF-BB antibody from 25 to 100 ng and then decreased slightly. Hence, 100 ng of PDGF-BB antibody amount was selected for the following studies. Second, it is essential to use blocking reagent to block the remaining NOS group after the coupling of PDGF-BB antibody to the 96-well plate. The incomplete blocking would generate a high background. Several kinds of blocking reagents were investigated, including casein, BSA, Tris, lysine and leucine (Fig. 2). Compared to macromolecule blockers, a relatively high CL intensity was obtained by using small molecule blockers. The highest signal/noise ratio was obtained using Tris as the blocking reagent. Thus, Tris was selected as blocking agent in the assay. Third, we employed 13-nm and 44-nm streptavidin–gold as the detector and tried to find out the optimum NP size for the assay (Fig. 3). The optimized concentration of 13-nm and 44-nm streptavidin–gold for the determination of PDGF-BB were 0.46 nM and 12 pM, respectively (data not shown). Compared to 44-nm streptavidin–gold, a better response signal was obtained using 13 nm of

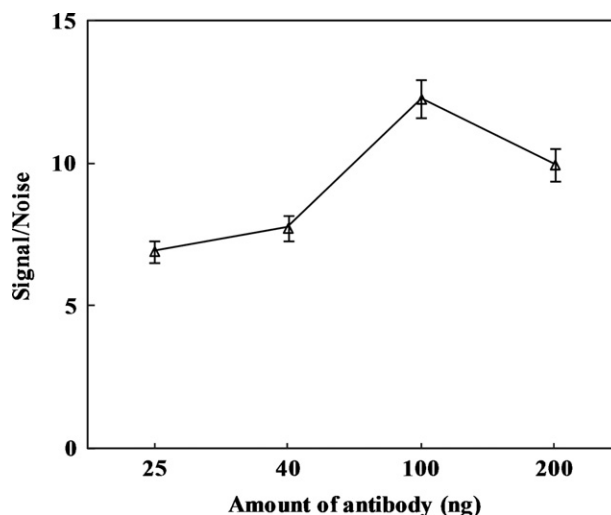


Fig. 1. Signal/noise vs. the amount of antibody. Experimental conditions: Tris, 10 mM; PDGF-BB, 6 nM; aptamer, 20 pmol; streptavidin–gold (13 nm), 1.392 nM;  $\text{HAuCl}_4$ , 0.25 mM;  $\text{NH}_2\text{OH}$ , 0.5 mM; the reduction time ( $T_R$ ), 6 min.

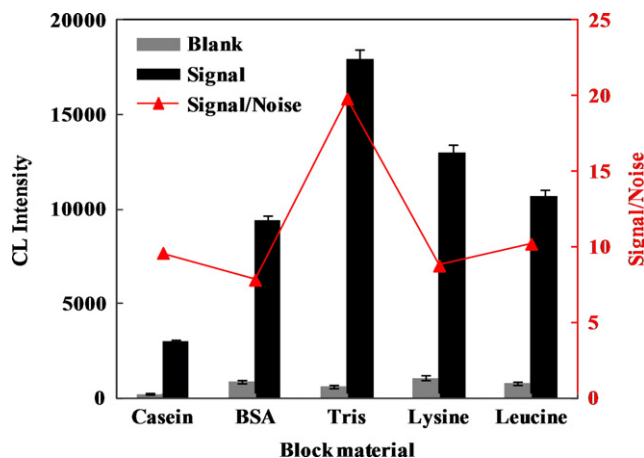


Fig. 2. Effect of block reagents on signal and background values. Experimental conditions: lysine, 10 mM; leucine, 10 mM; Tris, 10 mM; BSA, 2% (w/v); casein, 5% (w/v); antibody, 100 ng; streptavidin–gold (13 nm), 0.464 nM. Other experimental conditions were the same as Fig. 1.

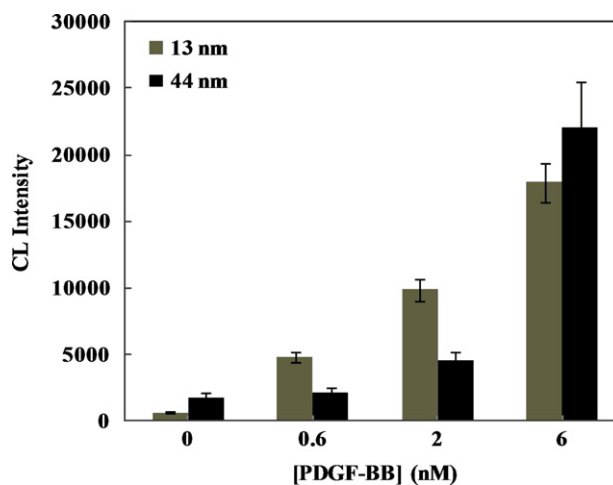


Fig. 3. Effect of gold size on the CL intensity. Experimental conditions: antibody, 100 ng; streptavidin–gold (13 nm), 0.464 nM; streptavidin–gold (44 nm), 0.012 nM. Other experimental conditions were the same as Fig. 1.

streptavidin–gold. We presumed that the Au-NPs with smaller size might show lower steric hindrance, therefore providing higher reaction efficiency between the biotin and streptavidin–gold. Hence, a higher signal was obtained by using smaller particle. Fourth, signal/noise ratio increased rapidly with the increase of biotinylated aptamer in the range of 5–20 pmol, indicating that a higher level of streptavidin–gold was captured on the plate surface. The signal/noise ratio decreased beyond 20 pmol of biotinylated aptamer, which was attributed to the increased background (Fig. 4). The signal/noise ratio was the highest at 20 pmol of biotinylated aptamer. Hence, 20 pmol of biotinylated aptamer was used for the following studies.

NH<sub>2</sub>OH was employed as the reducing agent in the signal amplification step where gold metal was catalytically deposited onto the surface of the Au NP labels. The concentration of NH<sub>2</sub>OH, HAuCl<sub>4</sub> and  $T_R$  affected the quantity of gold atoms deposited on the surface of the gold labels. First, signal/noise ratio increased rapidly with the extension of reduction time in the range from 0 to 4 min, and then decreased slightly. However, signal/noise ratio was the highest at 4 min (Fig. 5). Hence, the reduction time was set at 4 min. Second, as the concentration of HAuCl<sub>4</sub>

increased, the signal/noise ratio increased from 0.25 to 1 mM and then leveled off between 1–2 mM HAuCl<sub>4</sub> (Fig. 6). Thus, 1 mM HAuCl<sub>4</sub> was selected for the following experiments. Third, as shown in Fig. 7, 0.5 mM of NH<sub>2</sub>OH was selected for use in further studies.

### 3.3. Assay performance of detecting PDGF-BB

The quantitative behavior of the CL assay was assessed with different concentrations of PDGF-BB under the optimized conditions. From Fig. 8, it can be seen that the CL intensity increases with the increasing PDGF-BB concentration. A good linear relationship between the CL intensity and PDGF-BB concentration was observed in the range of 0.06–6 nM. The regression equation is  $I = 7436.3c - 1238$  (where  $c$  is the concentration of PDGF-BB, nM) with a correlation coefficient of 0.9945. From all studies done under optimized conditions, a detection limit, defined as the background signal plus three times its standard deviation of 60 pM, corresponding to 6 fmol in a 100  $\mu$ L volume was obtained. A series of seven repetitive measurements of PDGF-BB solution (0.2, 1 and 5 nM) yielded reproducible signals with a relative standard deviation of 9.5%, 6.7% and 3.5%, respectively.

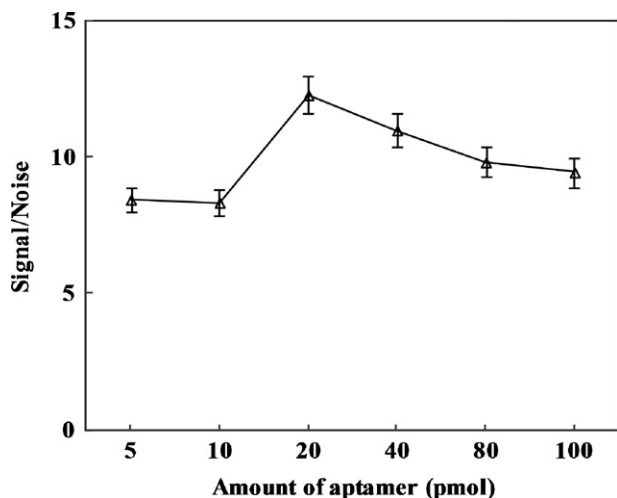


Fig. 4. Signal/noise vs. the amount of biotinylated aptamer. Experimental conditions: antibody, 100 ng; streptavidin–gold (13 nm), 0.464 nM. Other experimental conditions were the same as Fig. 1.

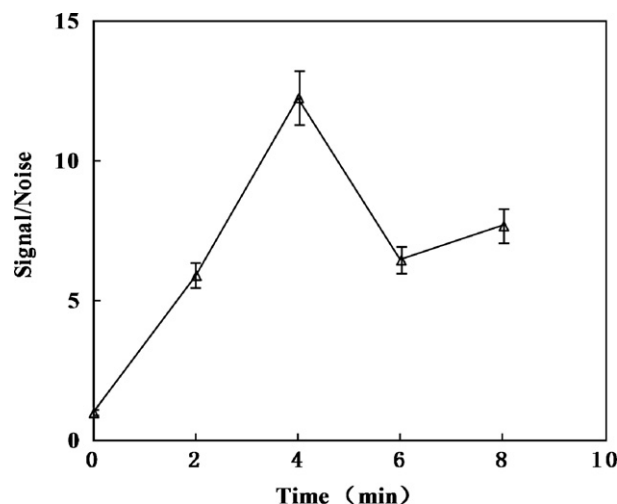


Fig. 5. Signal/noise vs.  $T_R$ . Experimental conditions: antibody, 100 ng; Tris, 10 mM; PDGF-BB, 6 nM; aptamer, 20 pmol; streptavidin–gold (13 nm), 0.464 nM; HAuCl<sub>4</sub>, 0.25 mM; NH<sub>2</sub>OH, 0.5 mM.

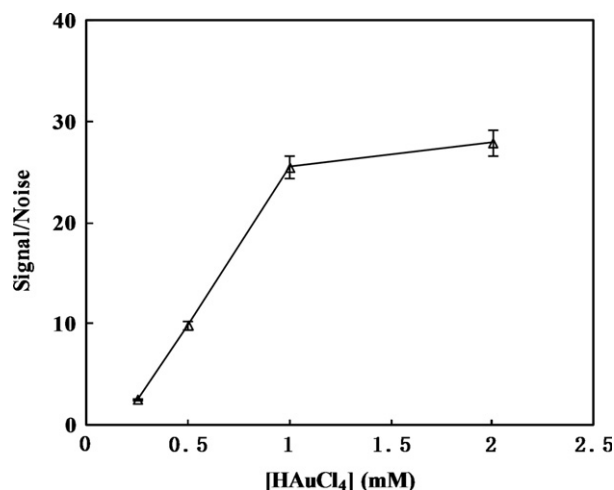


Fig. 6. Signal/noise vs. the concentration of HAuCl<sub>4</sub>. Experimental conditions: PDGF-BB, 2 nM;  $T_R$ , 4 min. Other experimental conditions were the same as Fig. 5.

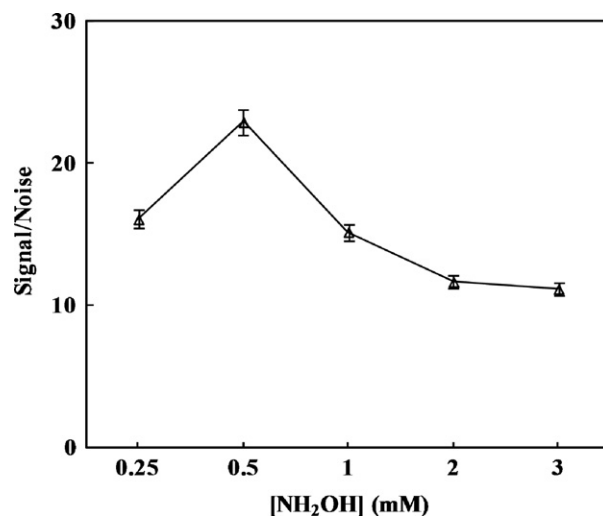
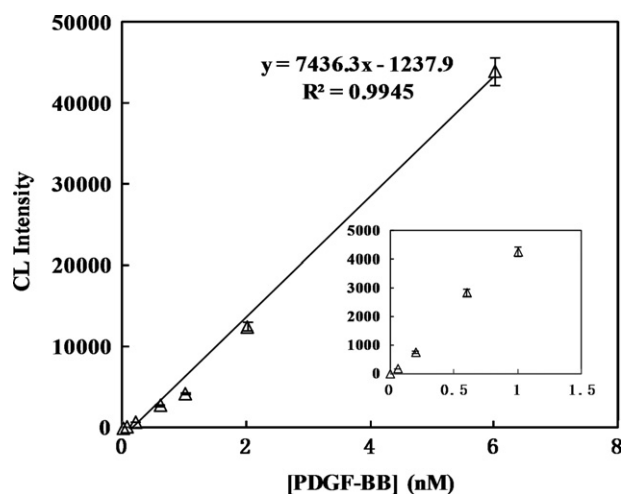
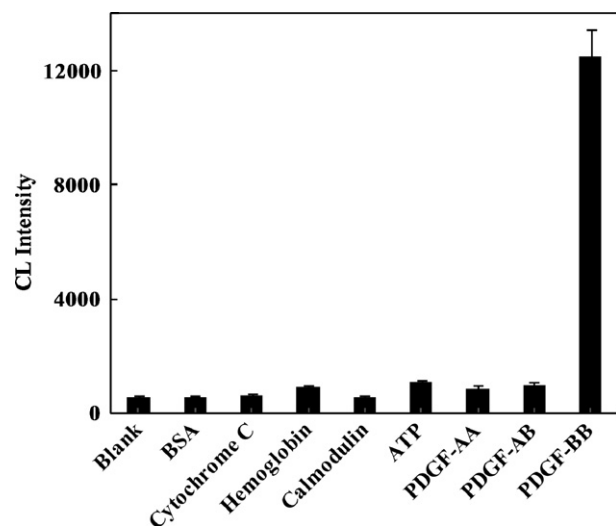


Fig. 7. Signal/noise vs. the concentration of NH<sub>2</sub>OH. Experimental conditions: HAuCl<sub>4</sub>, 1 mM;  $T_R$ , 4 min. Other experimental conditions were the same as Fig. 5.



**Fig. 8.** CL intensity vs. different concentrations of PDGF-BB. Experimental conditions:  $\text{NH}_2\text{OH}$ , 0.5 mM; PDGF-BB, 0, 0.06, 0.2, 0.6, 1, 2, 6 nM. Other experimental conditions were the same as Fig. 7. PDGF-BB concentrations of inset are 0, 0.06, 0.2, 0.6, and 1 nM.



**Fig. 9.** Specificity of the PDGF-BB assay detecting different target. PDGF-BB, 2 nM; PDGF-AA, 2 nM; PDGF-AB, 2 nM; BSA, 200 nM; hemoglobin, 200 nM; cytochrome C, 200 nM; calmodulin, 200 nM; ATP, 200 nM. Other experimental conditions were the same as Fig. 8.

Although the binding of the aptamer and the target protein is of high specificity, the non-specific adsorption of other proteins coexisting in the complex sample may possibly cause an interfering signal. Hence, the detection selectivity of the aptamer-based CL biosensor is an important criterion for its actual application. To evaluate the selectivity of the aptasensor, control experiments were performed using some potential interfering proteins including BSA, hemoglobin, cytochrome C, calmodulin, ATP, PDGF-AA, and PDGF-AB. As shown in Fig. 9, a high response was observed when 2 nM PDGF-BB was tested, whereas negligible signals were obtained in the absence of PDGF-BB and presence of 2 nM of PDGF-AA (or PDGF-AB), and 200 nM of BSA, hemoglobin, cytochrome C, calmodulin or ATP. Compared to previous reference in which a PDGF-B aptamer was used alone for the determination of PDGF [1], our method exhibits higher specificity to PDGF-BB. The other two PDGF isoforms (PDGF-AA and PDGF-AB) will not interfere with PDGF-BB detection, which is attributed to the combination of specific PDGF-B aptamer and anti-human PDGF-BB polyclonal antibody. The results suggest that the non-specific proteins do not interfere with PDGF-BB detection

obviously. This excellent selectivity indicates that it holds promise in the detection of PDGF-BB in complex samples.

### 3.4. Analysis of serum sample

Finally, the ability of the aptamer-based CL assay to detect PDGF-BB in complex matrixes was tested by using a standard addition method. A series of samples were prepared by adding known concentrations of PDGF-BB to 100-fold-diluted human serum. The recoveries of PDGF-BB from serum samples spiked with 0.2, 1, 5 nM were determined based on the calibration graph using PDGF-BB in PBSM at comparable levels ( $n=3$ ). The data for the quantization of PDGF-BB are shown in Table 1, which indicates recoveries ranging from 98.5% to 103.2%. PDGF-BB is an important cytokine, which has been implicated in the cell transformation process, glomerulonephropathy (IgAN), type 2 diabetes mellitus, and tumor growth and progression. For example, the levels of serum PDGF-BB in kidney cancer patients have been found in the sub-nanomolar range: 0.28–0.53 nM [29], which is significantly higher than that in health subjects ( $36 \pm 4$  pM). The local PDGF concentration in a tumor area is expected to be higher than that in the blood samples as a result of its dilution in blood and short lifetime in circulation [30]. We expect that the sensitivity and concentration range of PDGF-BB detection achieved in this study will be suitable for potential application in the preliminary diagnosis of cancer.

## 4. Conclusion

In conclusion, we have developed a sandwich assay for PDGF-BB by taking advantage of aptamer for the increased specificity, the use of hydroxylamine-amplified Au NPs for signal amplification, and CL technique for highly sensitive detection. The hydroxylamine-amplified Au NPs-based aptameric CL biosensor demonstrated high sensitivity that can detect the presence of

**Table 1**  
Recovery of PDGF-BB spiked into human serum samples.

Amount added (nM)	Amount measured (nM)	Recovery (%)
0.2	$0.197 \pm 0.006$	$98.5 \pm 2.9$
1	$1.014 \pm 0.085$	$101.4 \pm 8.5$
5	$5.162 \pm 0.354$	$103.2 \pm 7.1$

**Table 2**  
Comparison of sensitivity for different PDGF-BB assay methods.

Analytical method	Label	Detection limit	Linearity range
Electrochemical assay [31]	Silver deposition	10 fM	10 fM–100 pM
Electrochemical assay [32]	Ferrocene	36 fM	41 fM–820 pM
Colorimetric assay [1]	Au	0.3 nM	0.5–20 nM
Colorimetric assay [21]	ABTS	8.2 fM	41 fM–4.1 pM
Fluorescence assay [15]	Cy5	4 pM	4 pM–100 nM
Capillary electrophoresis [33]		50 pM	0.5–50 nM
CL detection [34]	$[\text{Ru}(\text{phen})_2(\text{dppz})]^{2+}$	1 nM	0–50 nM
CL detection (this study)	Au NPs	60 pM	0.06–6 nM
ECL detection [35]	$\text{Ru}(\text{bpy})_3^{2+}$	80 pM	0.1–1000 nM



PDGF-BB at a concentration as low as 60 pM (corresponding to 6 fmol in a 100  $\mu$ L volume), which compares favorably with those of other PDGF-BB detection techniques (Table 2). In addition, this aptameric CL biosensor also demonstrated extraordinary specificity. And PDGF-BB has been determined in diluted serum, indicating the applicability of this assay. The proposed protocol can potentially become a powerful tool for protein detection due to the wide availability of aptamer for numerous proteins.

## Acknowledgments

This study was supported by the National Natural Science Foundation of China (21105071), the Specialized Research Fund for the Doctoral Program of Higher Education of China (20110032120079) and the Innovation Foundation of Tianjin University (2010XJ-0167).

## References

- [1] T.E. Lin, W.H. Chen, Y.C. Shang, C.C. Huang, H.T. Chang, *Biosens. Bioelectron.* 29 (2011) 204–209.
- [2] J. Lee, K. Icoz, A. Roberts, A.D. Ellington, C.A. Savran, *Anal. Chem.* 82 (2010) 197–202.
- [3] Z.S. Wu, H. Zhou, S.B. Zhang, G.L. Shen, R.Q. Yu, *Anal. Chem.* 82 (2010) 2282–2289.
- [4] S.Y. Yan, R. Huang, Y.Y. Zhou, M. Zhang, M.G. Deng, X.L. Wang, X.C. Weng, X. Zhou, *Chem. Commun.* 47 (2011) 1273–1275.
- [5] R.H. Yang, Z.W. Tang, J.L. Yan, H.Z. Kang, Y.M. Kim, Z. Zhu, W.H. Tan, *Anal. Chem.* 80 (2008) 7408–7413.
- [6] D.Y. Liu, Y. Zhao, X.W. He, X.B. Yin, *Biosens. Bioelectron.* 26 (2011) 2905–2910.
- [7] G. Pelossof, R. Tel-Vered, J. Elbaz, I. Willner, *Anal. Chem.* 82 (2010) 4396–4402.
- [8] B.J. Shen, Q. Wang, D. Zhu, J.J. Luo, G.F. Cheng, P.G. He, Y.Z. Fang, *Electroanalysis* 22 (2010) 2985–2990.
- [9] G.Q. Wen, L.P. Zhou, T.S. Li, A.H. Liang, Z.L. Jiang, *Chin. J. Chem.* 30 (2012) 869–874.
- [10] Q. Chen, W. Tang, D.Z. Wang, X.J. Wu, N. Li, F. Liu, *Biosens. Bioelectron.* 26 (2010) 575–579.
- [11] Y.K. Jung, T.W. Kim, H.G. Park, H. Tom Soh, *Adv. Funct. Mater.* 20 (2010) 3092–3097.
- [12] L.S. Selvakumar, M.S. Thakur, *Anal. Biochem.* 427 (2012) 151–157.
- [13] H.A. Ho, M. Leclerc, *J. Am. Chem. Soc.* 126 (2004) 1384–1387.
- [14] C.H. Heldin, *EMBO J.* 11 (1992) 4251–4259.
- [15] A.R. Ruslinda, V. Penmats, Y. Islili, S. Tajinma, H. Kawarada, *Analyst* 137 (2012) 1692–1697.
- [16] W.Q. Song, K.L. Zhu, Z.J. Cao, C.W. Lau, J.Z. Lu, *Analyst* 137 (2012) 1396–1401.
- [17] K.J. Feng, L.P. Qiu, Y. Yang, Z.S. Wu, G.L. Shen, R.Q. Yu, *Biosens. Bioelectron.* 29 (2011) 66–75.
- [18] Y. Chai, D.Y. Tian, J. Gu, H. Cui, *Analyst* 136 (2011) 3244–3251.
- [19] D.B. Zhu, X.M. Zhou, D. Xing, *Anal. Chim. Acta* 725 (2012) 39–43.
- [20] Y. Huang, X.M. Nie, S.L. Gan, J.H. Jiang, G.L. Shen, R.Q. Yu, *Anal. Biochem.* 382 (2008) 16–22.
- [21] L.H. Tang, L. Yang, M.M. Ali, D.K. Kang, W.A. Zhao, J.H. Li, *Anal. Chem.* 84 (2012) 4711–4717.
- [22] J.S. Li, T. Deng, X. Chu, R.H. Yang, J.H. Jiang, G.L. Shen, R.Q. Yu, *Anal. Chem.* 82 (2010) 2811–2816.
- [23] S. Bi, Y.M. Yan, X.Y. Yang, S.S. Zhang, *Chem. Eur. J.* 15 (2009) 4704–4709.
- [24] A.P. Fan, C. Lau, J.Z. Lu, *Analyst* 134 (2009) 497–503.
- [25] M.C. Daniel, D. Astruc, *Chem. Rev.* 104 (2004) 293–346.
- [26] G. Frens, *Nat. Phys. Sci.* 241 (1973) 20–22.
- [27] C. Guarise, L. Pasquato, V. De Filippis, P. Scrimin, *Proc. Natl. Acad. Sci. USA* 103 (2006) 978–9982.
- [28] Y.J. Niu, Y.J. Zhao, A.P. Fan, *Anal. Chem.* 83 (2011) 7500–7506.
- [29] J. Guo, Y.F. Cao, *Pract. Clin. Med.* 9 (2008) 29–31.
- [30] J.P. Singh, M.A. Chaikin, C.D. Stiles, *Cell Biol.* 95 (1982) 667–671.
- [31] L. Zhou, L.J. Ou, X. Chu, G.L. Shen, R.Q. Yu, *Anal. Chem.* 79 (2007) 7492–7500.
- [32] Y.L. Zhang, Y. Huang, J.H. Jiang, G.L. Shen, R.Q. Yu, *J. Am. Chem. Soc.* 129 (2007) 15448–15449.
- [33] H. Zhang, X.F. Li, X.C. Le, *Anal. Chem.* 81 (2009) 7795–7800.
- [34] Y. Jiang, X. Fang, C. Bai, *Anal. Chem.* 76 (2004) 5230–5235.
- [35] D.B. Zhu, X.M. Zhou, D. Xing, *Biosens. Bioelectron.* 26 (2010) 285–288.